phys. stat. sol. (a) **179**, 285 (2000)

Subject classification: 73.40.Kp; 77.65.Ly; 77.70.+a; S7.14

Novel Nitride Devices Based on Polarization Fields[1])

J. A. MAJEWSKI[2]), G. ZANDLER, and P. VOGL

Walter Schottky Institute, Technical University of Munich, Am Coulombwall, D-85748 Garching, Germany

(Received March 17, 2000)

A key property of the nitrides is the fact that they possess large spontaneous and piezoelectric polarization fields that allow a significant tailoring of the carrier dynamics and optical properties of nitride devices. In this paper, based on first-principles calculations of structural and electronic properties of bulk nitrides and their heterostructure, we investigate the potential of this novel material class for modern device applications by performing self-consistent Monte Carlo simulations. We demonstrate that the internal electric fields have a significant and favorable influence on the transistor characteristics.

1. Introduction

The strong internal electric fields in nitrides that result from their strong pyro- and piezoelectric constants [1] have a dramatic effect on the electronic and optical properties in these systems. In the GaN or InGaN quantum wells, the electric field in the well causes the red shift of transition energies and strongly supresses the interband transitions [2]. This effect is generally considered as unfavorable for the optoelectronic devices based on multiple quantum wells [3]. On the other hand, the electric fields increase the electron and/or hole densities accumulated at the interfaces. This opens new possibilities for device engineering. In the present paper, we demonstrate how the pyro- and piezoelectric character of the nitrides can be utilized in the design of the novel heterostructure field effect transistors (HFETs). We show that the internal electric fields have a significant and favorable influence on the transistor characteristics. So far, only few theoretical predictions on the carrier dynamics in nitride devices have been published [4].

2. Theory of Internal Polarization Fields in GaN and AlN Interfaces

In this section, we discuss the influence of the polarization fields on properties of nitride heterostructures. The present systematic theoretical studies of structural and electronic properties of heteroepitaxial AlN/GaN interfaces and homoepitaxial stacking faults [5], are based on a well-established first-principles total-energy pseudopotential method within the local-density-functional formalism [6]. The band offsets, the charge accumulation at the polar interfaces of the junctions, and the interface electronic states have been investigated, taking fully into account the effects of lattice relaxation and electric polarization.

[1]) Presented at the 216th WE-Heraeus Seminar in Ilmenau, May 31 to June 2, 1999, "Nitrogen in Solids and at Solid Surfaces: Present Status and Future Trends".

[2]) Corresponding author: Fax: ++49-89-28912737; e-mail: majewski@wsi.tu-muenchen.de

2.1 Polarity of interfaces

The space group P6$_3$mc (C_{6v}^4) of wurtzite structure is compatible with a spontaneous polarization along the hexagonal *c*-axis. Therefore, the polarization can be of both pyroelectric and piezoelectric origin in wurtzite AlN and GaN, but only piezoelectric in the cubic phases. Whenever the polarization lies parallel to the growth direction, its change (divergence) across the interface is equivalent to an interface charge. Among the interfaces between GaN and AlN that we have studied, the [111] GaN/AlN, the [0001] GaN/AlN, and the stacking fault interface between the wurtzite and zincblende GaN interface are of this type, which may be termed "polar". In cases such as [$\bar{1}2\bar{1}0$] GaN/AlN, [$0\bar{1}10$] GaN/AlN, or [110] GaN/AlN, on the other hand, the polarization lies parallel to the interface and therefore does not give rise to a charge accumulation. We term those interfaces "nonpolar". A limiting case of this type is the cubic [001] GaN/AlN interface.

2.2 Internal polarization fields in quantum wells

Most of the optoelectronic and electric nitride devices are based on the quantum wells. In such a structure, a thin layer of one semiconductor (e.g., GaN) constituing the well is embedded in another material (e.g., AlGaN). The vector of electric polarization in each material (i = 1,2) can be written as $\mathbf{P}^{(i)} = \mathbf{P}_0^{(i)} + \chi^{(i)}\ \mathbf{E}^{(i)}$, where zero field polarization $\mathbf{P}_0^{(i)}$ consists of spontaneous and/or piezoelectric polarization, and $\chi^{(i)}$ is the susceptibility of material "i". The most interesting case is when the polarizations $\mathbf{P}_0^{(i)}$ are perpendicular to the interfaces (like in the [0001] GaN/AlN system, for example). Then the divergence of the polarizations in two semiconductors gives rise to the polarization charges at the interfaces σ and further to the electric fields $\mathbf{E}^{(i)}$. The interface charge and electric field in the well are dependent on the boundary conditions imposed on the system. Here we consider three types of boundary conditions: (i) free standing system in vacuum, (ii) periodic boundary conditions, i.e., the potentials of the external surfaces of the cladding layers are equal, and (iii) neutralizing free charges σ_{fL} and σ_{fR} at the external surfaces. Further, we assume that the well has thickness l_1 and the two cladding layers on both sides of the well have thickness l_2 each. Using simple electrostatic arguments and considering the boundary conditions for the normal components of the electric displacements $D^{(i)} = 4\pi P_0^{(i)} + \epsilon_i E^{(i)}$ (ϵ_i dielectric constant) at four interfaces (two external surfaces and two internal interfaces) for the cases (i) to (iii), one obtains the interface polarization charges $\pm\sigma$ and electric fields in the well ($E^{(1)}$) and the cladding layers ($E^{(2)}$):

$$\text{(i)}\quad \sigma = \frac{P_0^{(2)}}{\epsilon_2} - \frac{P_0^{(1)}}{\epsilon_1}\,; \qquad E^{(1)} = -\frac{4\pi P_0^{(1)}}{\epsilon_1}\,; \qquad E^{(2)} = -\frac{4\pi P_0^{(2)}}{\epsilon_2}\,, \tag{1}$$

$$\text{(ii)}\quad \sigma = \frac{\left(P_0^{(2)} - P_0^{(1)}\right)(2l_2 + l_1)}{2l_2\epsilon_1 + l_1\epsilon_2}\,; \qquad E^{(1)} = 4\pi\sigma\frac{2l_2}{2l_2 + l_1}\,; \qquad E^{(2)} = -E^{(1)}\frac{l_1}{2l_2}\,, \tag{2}$$

$$\text{(iii)}\quad \sigma = \frac{P_0^{(2)} - P_0^{(1)}}{\epsilon_1}\,; \qquad E^{(1)} = 4\pi\sigma\,; \qquad E^{(2)} = 0\,. \tag{3}$$

Note that the relation $E^{(1)} - E^{(2)} = 4\pi\sigma$ holds in all three cases. In the case (iii), the free surface charges that cause the electric field in the cladding layer to vanish are

$\sigma_{fL} = -\sigma_{fR} = P_0^{(2)}$. In the case (ii), the fields $E^{(1)}$, $E^{(2)}$, and the interface charge σ tend to the corresponding quantities from the case (iii), if the cladding layer thickness increases to infinity ($l_2 \to \infty$). For semiconductors with very similar dielectric constants ($\epsilon_1 \approx \epsilon_2$), like in the case of AlGaN/GaN quantum wells, the interface polarization charges are independent of the boundary conditions at the external surfaces. Then, the quantum well with neutralized surface charges (i.e., $E^{(2)} = 0$) can be well simulated in supercell calculations with periodic boundary conditions.

2.3 GaN/AlN heterostructures

In the following, we consider strained GaN layers that are grown pseudomorphically on cubic or wurtzite AlN substrate. For cubic heterostructures, we consider [001], [110], and [111], and for the wurtzite heterostructures [0001], $[0\overline{1}10]$, and $[\overline{1}2\overline{1}0]$ growth directions. In the case of stacking fault interfaces, we assume the growth axis to be the hexagonal *c*-axis ([0001] in wurtzite, [111] in zincblende).

Computationally, we have modeled all of these interfaces by supercells containing up to 40 atoms (for $[0\overline{1}10]$ and $[\overline{1}2\overline{1}0]$ wurtzite structures). All atomic positions in the unit cell have been optimized by minimizing the total energy via the Hellmann-Feynman forces. The length of the supercell was determined by minimizing the stress tensor component along the growth direction. Based on these first-principles calculations, we find that the charges induced at the interfaces and VBOs are insensitive to the lattice constant along the growth direction, but highly sensitive to the atomic relaxation at the interface (e.g. the VBO for the relaxed [0001] GaN/AlN interface is 0.4 eV smaller than for the unrelaxed one). The lattice relaxation near the interface reduces the interface charge approximately by a factor of two.

2.4 Valence band offsets and interface charges

The valence band offset ΔE_V at an interface between two semiconductors (or between two phases of one material) can be conveniently split up into two terms [7] $\Delta E_V = \Delta\overline{V} + \Delta E_{BS}$, where $\Delta\overline{V}$ is the asymptotic difference between the laterally and vertically averaged electrostatic potential $\overline{V}(z)$, and ΔE_{BS} is the bulk band structure contribution. For neutral interfaces, $\Delta\overline{V}$ equals the dipole moment of the electrostatic charge density $\overline{\rho}(z)$ across the interface. In the case of charged interfaces, the electrostatic charge density $\overline{\rho}(z)$ contains an additional monopole term that is proportional to the difference between the polarizations in the two adjacent materials. The monopole charge density causes the macroscopically averaged electrostatic potential to change linearly with distance from the interface. This contribution can be filtered out [8] and the intrinsic $\Delta\overline{V}$ can be obtained, based on the remaining dipolar contribution to $\overline{\rho}(z)$. By integrating the monopole charge density across the interface, we have been able to calculate the charge induced at the interface σ. Finally, the conduction band offset ΔE_C is defined by $\Delta E_C = \Delta E_V + \Delta E_{gap}$, where ΔE_{gap} is the difference between the fundamental band gaps of two constituent bulk crystals.

The calculated band offsets and charges induced at polar interfaces are given in Table 1, together with the individual contributions to the VBOs. The band lineups of the studied heterostructures are depicted also in Fig. 1. The presently predicted VBOs agree very well with recent experimental data [9, 10], but not with some core-level photoemission data that suggest an extremely high VBO of 1.36 eV [11].

Table 1
Valence and conduction band offsets ΔE_V [eV] and ΔE_C [eV], potential lineups $\Delta\overline{V}$ [eV], band structure contributions ΔE_{BS} [eV], and interface charge σ [C/m^2] for GaN/AlN heterostructures and stacking fault interfaces. For GaN/AlN heterostructures, all values are given relative to the band edges in AlN, whereas for stacking faults they are given relative to the band edges of the wurtzite phase. The conversion factor for σ (C/m^2 to cm^{-2}) is 6.241×10^{14}

	wurtzite GaN/AlN			zincblende GaN/AlN			stacking faults	
	[0001]	[0$\bar{1}$10]	[$\bar{1}$2$\bar{1}$0]	[001]	[110]	[111]	AlN	GaN
ΔE_{BS}	−0.26	−0.15	−0.17	−0.15	−0.15	0.13	−0.25	−0.046
$\Delta\overline{V}$	0.93	0.88	0.97	0.89	1.07	0.77	0.27	0.081
ΔE_V	0.67	0.73	0.80	0.75	0.92	0.90	0.02	0.04
ΔE_C	−1.92	−1.72	−1.67	−0.62	−0.51	−0.53	−1.30	−0.17
σ	0.010	0	0	0	0	0.006	0.009	0.003

It is interesting to note that all calculated VBOs are of the order of 0.7 to 0.9 eV and are insensitive to the polar/nonpolar character of the interface. Thus, the macroscopic electric fields do not grossly alter or modify the intrinsic band offsets. The large difference between conduction band offsets in cubic and wurtzite GaN/AlN heterostructures is a consequence of the indirect energy gap ($\Gamma \rightarrow X$) in cubic AlN that is 1.4 eV smaller than the direct gap in wurtzite AlN.

All studied GaN/AlN interfaces and stacking faults are of type I, with the valence band lying higher and the conduction band being lower in GaN, and zincblende phase of the stacking fault, respectively. The large charges accumulated at the stacking fault interfaces result mainly from the spontaneous dielectric polarization of the hexagonal phase, whereas the strain-induced piezoelectric contribution is negligible. The induced charges are seen to be reduced by a factor of two by the relaxation of the atomic positions at the interface. The presently calculated charges compare well (the difference amounts to 15 to 20 %) with results obtained from electrostatic arguments (Eqs. (2) and (3)), in which the bulk values of the spontaneous polarization, and piezoelectric constants [1] have been used. The stacking faults can generate a persistent photoconductivity and they can be tuned to act either as excitonic traps or luminescence centers, depending on the width of the cubic layer.

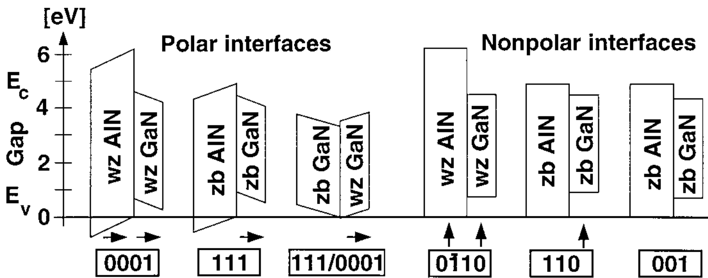

Fig. 1. Predicted band lineups for several AlN/GaN interfaces. The growth direction is given in boxes beneath each interface. The arrows indicate the direction of the spontaneous or strain-induced piezoelectric polarization. Polar interfaces possess an interface charge. The corresponding electric field induces a band bending that is indicated schematically

Our calculations reveal the existence of large internal electric fields. Their influence on the properties of the electronic devices will be presented in subsequent sections.

3. Monte Carlo Calculations

Before we turn to the heterostructure based transistors, let us shortly discuss the transport properties of bulk nitrides.

3.1 Bulk transport properties of GaN and AlN

In our Monte Carlo transport calculations, we have used band parameters [12] deduced from the electronic structure calculations described above and have taken into account scattering rates for ionized impurity, intra- and intervalley phonon scattering, acoustic, piezoelectric, polar optical phonon and alloy scattering. The resulting electron drift velocities (see Fig. 2) at room temperature in bulk GaN both at low and high fields are in good agreement with other published theoretical results [13]. At high fields, GaN as well as AlN show a saturation velocity ($\approx 1.5 \times 10^7$ cm/s at 1 MV/cm) that is twice as high as in GaAs. For AlN, the heavier effective mass leads to considerably lower drift velocities at low fields. These results indicate that one can achieve much higher transit time frequencies in sub-micron nitride devices than in GaAs ones.

3.2 Polarization fields in wurtzite AlGaN/GaN single heterostructures

As discussed in Section 2, the electric polarization in nitride structures induces the polarization charge at the heterostructure interface. To study the effect of this interface charge on carrier transport and heterostructure device characteristics, we focus on a single $Al_{0.15}Ga_{0.85}N$/GaN heterostructure (see Fig. 3) first. In a tensile strained 30 nm thick $Al_{0.15}Ga_{0.85}N$ layer on GaN substrate, there is polarization of both pyro- and piezoelectric origins, while the relaxed 300 nm thick GaN layer contains the pyroelectric moment only. We assume that there are some compensating charges at the surface and the nucleation layer. The polarization charge at the $Al_{0.15}Ga_{0.85}N$/GaN interface has been taken to be 6×10^{12} cm^{-2}, which interpolates between a recent experimental value [14] 4×10^{12} cm^{-2} and the theoretical value 8×10^{12} cm^{-2} calculated for full compensation.

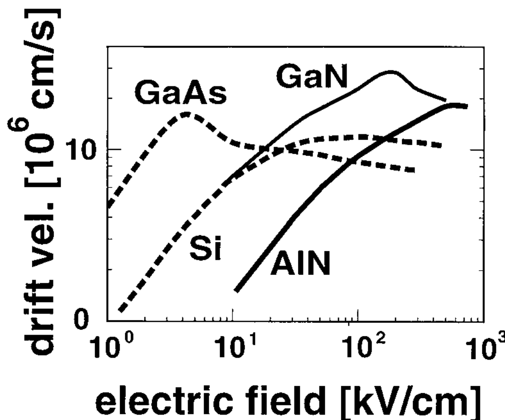

Fig. 2. Calculated electron drift velocities of GaN and AlN in comparison with that of GaAs and Si

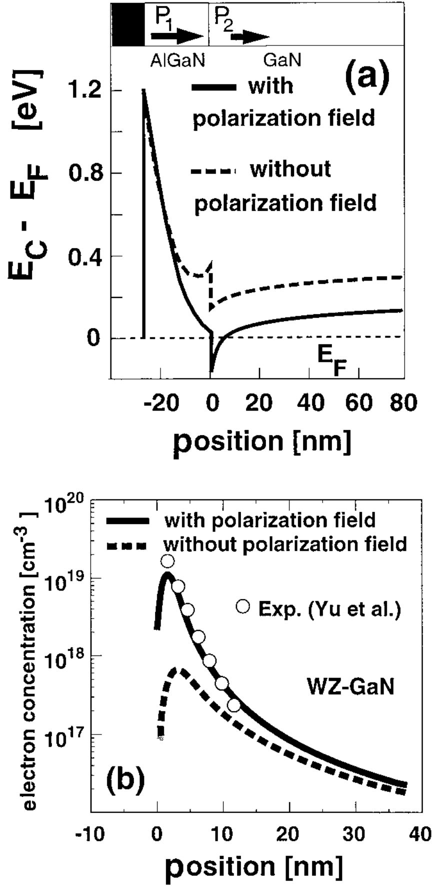

Fig. 3. Calculated results for a $Al_{0.15}Ga_{0.85}N/GaN$ HFET with (full lines) and without (dashed lines) spontaneous and piezoelectric fields. A homogeneous n-doping background of 10^{16} cm^{-3} throughout the structure has been assumed. a) Self-consistently computed conduction band edge profile along the growth direction. b) Calculated electron density profile in comparison with published experimental values

Figure 3 depicts the self-consistent band edge and density profiles along the growth direction obtained from the coupled one-dimensional Schrödinger and Poisson equations. The Poisson equation includes all interface charges that result from the polarization fields. As shown in Fig. 3, the polarization induced positive interface charge causes a stronger confinement of two-dimensional (2D) electron channel and an increase in the channel density by more than an order of magnitude. This is consistent with the experimental values for this layer structure [14].

Furthermore, we have performed ensemble Monte Carlo calculations for drift mobilities along the channel that forms parallel to the interface. The inter- and intra-subband-scattering rates [15] have been determined consistently with the confined electronic channel states. We find excellent agreement between experimental and calculated temperature dependent mobilities [15], consistent with the high channel densities reported for these devices [14,16]. We would like to stress that such type of agreement strongly supports the existence of the strong pyroelectric polarization fields. For channel densities exceeding 10^{13} cm^{-2}, we predict a phonon limited drift mobility for 2D electrons close to 2000 cm^2/Vs for high quality interfaces, in good agreement with recent data on such structures [17].

3.3 Influence of polarization fields on device performance

To study the influence of polarization fields on device characteristics, we have performed self-consistent two-dimensional Monte Carlo simulations of various nitride based heterostructure devices [12]. At high bias voltages, it suffices to use a bulk description for the hot carrier transport in the channel layers.

In accordance with the high channel densities, the drain currents in such devices can become extraordinarily high. We have studied a 300 nm gate length single heterostructure device with the same layer sequence as described above, but with additional dop-

ing densities of 10^{18} cm^{-3} in the supply layer. This results in channel densities of 8×10^{12} cm^{-2} in the ungated structure. For this device, we find drain currents at open channel conditions up to 2000 A/m and predict a maximum transconductance of 430 S/m. Although the polarization induced interface charge in these devices suppresses parasitic substrate currents very efficiently, the magnitude of the threshold voltage is still fairly high (−6 V), mainly as a consequence of the high gate to channel separation of 30 nm.

Based on these bulk results, we have carried out self-consistent Monte Carlo simulations for planar short channel HFETs (heterostructure field effect transistors) [18]. We predict the following layer sequence to be well suited for high speed power applications. Beneath the contacts, we assume a highly doped $Al_{0.16}Ga_{0.84}N$ supply layer of 10 nm (4 nm with $n = 1 \times 10^{18}$ cm^{-3} and 6 nm with $n = 1 \times 10^{19}$ cm^{-3}). This is followed by an 8 nm $In_{0.05}Ga_{0.95}N$ channel with $n = 3 \times 10^{18}$ cm^{-3} and a subsequent 400 nm buffer layer that consists of $Al_{0.16}Ga_{0.84}N$. We assume this buffer layer to be fully compensated/nearly intrinsic, except for the first 6 nm that we take to be n-type with $n = 2 \times 10^{18}$ cm^{-3}. The intrinsic buffer is a prerequisite for obtaining an acceptable off-characteristics.

The influence of the polarization field on the drain current characteristics of a 300 nm gate HFET is shown in Fig. 4. The polarization field pushes the electrons closer to the gate contact and therefore increases the transconductance from 650 to 980 S/m. Furthermore, this confining effect improves the turn off behavior of the device considerably.

The present Monte Carlo calculations predict average channel velocities exceeding 2×10^5 m/s for gate lengths below 200 nm and yield transit time frequencies of 120 GHz for gate lengths between 200 and 300 nm and up to 300 GHz for 100 nm gate length. Velocity overshoot is found to remain small in all of these cases but the turn-off behavior is poor for very short gate lengths. These short channel effects become even more pronounced at elevated tem-

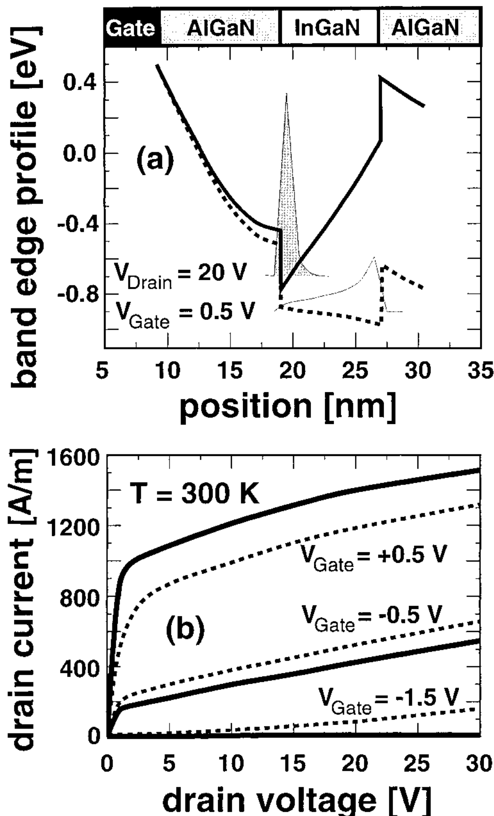

Fig. 4. Simulation results for a 300 nm gate length $In_{0.05}Ga_{0.95}N/Al_{0.16}Ga_{0.84}N$ HFET with (full lines) and without (dashed lines) spontaneous and piezoelectric fields. a) Self-consistent conduction band edge profile and electron density. b) Calculated drain current versus drain voltage for different gate voltages

peratures. In conlusion, we predict excellent high frequency and power performance for wide-gap nitride based HFETs with gate lengths larger than 200 nm.

Polarization induced internal fields can be effectively utilized to tailor devices with optimal potential barriers towards the substrate. Indeed, we have theoretically designed the following inverted HEMT structure that should yield high channel densities and an excellent turn-off behavior. On top of a relaxed GaN buffer, there is a 12 nm thick strained $Al_{0.40}Ga_{0.60}N$ layer. The inner part (8 nm) of this layer is highly n-doped with 1.9×10^{19} cm^{-3}. The remaining part of the barrier is moderately doped with 10^{17} cm^{-3} carriers. On top of this layer, there is a 30 nm GaN (n-doped with 4×10^{16} cm^{-3}). The gate is assumed to be recessed in order to achieve a small gate to channel separation of 14 nm. In this HFET, we assume the opposite polarity of the structure as in the previous example. The GaN is assumed to be field free, whereas two GaN/AlGaN interfaces have opposite interface charges equal to $\pm 2 \times 10^{13}$ cm^{-2}. The calculated band edge profile, together with the confined electron density is shown in Fig. 5a at midgate position.

As can be seen from Fig. 5, the polarization induced field produces a high potential barrier of approximately 3 eV towards the substrate. This has two major consequences. First, the highly doped AlGaN barrier gets completely depleted and all electrons are strongly confined in the channel that forms at the interface with the top GaN layer.

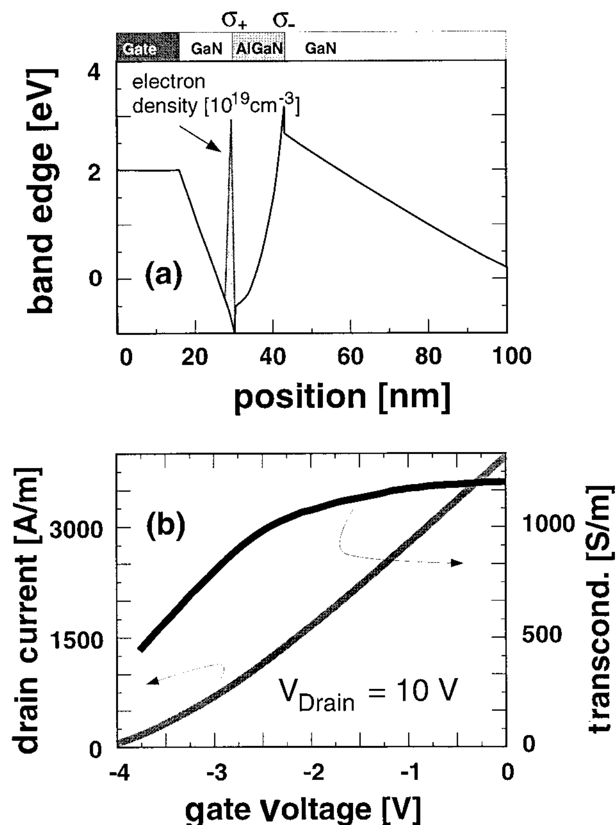

Fig. 5. Monte Carlo results for a 300 nm gate length inverted $GaN/Al_{0.40}Ga_{0.60}N$ HFET.
a) Self-consistent band edge profile for -1 V gate voltage and 10 V drain voltage. The channel electron density is indicated schematically. b) Drain current and transconductance versus gate voltage at 10 V drain voltage

Secondly, the high barrier completely suppresses the leakage current across the AlGaN barriers up to high voltages. We predict excellent electrical characteristics for such types of devices. In the present example, we find drain currents exceeding 3000 A/m and a transconductance that lies well above 1000 S/m. We note that the thickness of the AlGaN barrier layer and its doping level must be chosen carefully in order to avoid the formation of parasitic hole channels.

4. Conclusions

In conclusion, pyro- and piezoelectrical polarizations must be taken into account in order to explain experimentally observed mobilities and densities in nitride heterostructures. They are crucial for device performances and offer a unique possibility to design novel high power high frequency heterostructure transistors.

Acknowledgements This work has been supported by the Deutsche Forschungsgemeinschaft and the Bayerischer Forschungsverbund (FOROPTO).

References

[1] F. Bernardini, V. Fiorentini, and D. Vanderbilt, Phys. Rev. B **56**, 10024 (1997).
[2] M. Leroux, N. Grandjean, M. Laügt, J. Massies, B. Gil, P. Lefebvre, and P. Bigenwald, Phys. Rev. B **58**, 13371 (1998).
[3] M. B. Nardelli, K. Rapcewicz, and J. Bernholc, Appl. Phys. Lett. **71**, 3135 (1997).
[4] J. A. Majewski, G. Zandler, and P. Vogl, Semicond. Sci. Technol. **13**, 90 (1998).
[5] X. H. Wu, L. M. Brown, D. Kapolnek, S. Keller, B. Keller, S. P. Denbaars, and J. S. Speck, J. Appl. Phys. **80**, 3228 (1996).
[6] M. Städele, J. A. Majewski, and P. Vogl, Phys. Rev. B **56**, 6911 (1997).
J. A. Majewski, M. Städele, and P. Vogl, MRS Internet J. Nitride Semicond. Res. **1**, 30 (1996).
[7] A. Baldereschi, S. Baroni, and R. Resta, Phys. Rev. Lett. **61**, 734 (1988).
[8] F. Bernardini and V. Fiorentini, Phys. Rev. B **57**, R9427 (1998).
[9] G. Martin, A. Botchkarev, A. Rockett, and H. Morkoç, Appl. Phys. Lett. **68**, 2541 (1996).
[10] G. Martin, S. Strite, A. Botchkarev, A. Agarwal, A. Rockett, H. Morkoç, W. R. L. Lambrecht, and B. Segall, Appl. Phys. Lett. **65**, 610 (1994).
[11] J. R. Waldrop and R. W. Grant, Appl. Phys. Lett. **68**, 2879 (1996).
[12] G. Zandler, J. A. Majewski, M. Städele, P. Vogl, and F. Compagnone, phys. stat. sol. (b) **204**, 133 (1997).
[13] U. V. Bhapkar and M. S. Shur, J. Appl. Phys. **82**, 1649 (1997).
S. K. O'Leary, B. E. Foutz, M. S. Shur, U. V. Bhapkar, and L. F. Eastman, Solid State Commun. **105**, 621 (1988).
[14] E. T. Yu, G. J. Sullivan, P. M. Asbeck, C. D. Wang, D. Qiao, and S. S. Lau, Appl. Phys. Lett. **71**, 2794 (1997).
[15] R. Oberhuber, G. Zandler, and P. Vogl, Appl. Phys. Lett. **73**(6), 818 (1998).
[16] Y. F. Wu, B. P. Keller, D. Kapolnek, P. Kozodoy, S. P. Denbaars, and U. K. Mishra, Appl. Phys. Lett. **69**, 1438 (1996).
[17] R. Gaska, J. W. Yang, A. Osinsky, Q. Chen, M. A. Khan, A. O. Orlov, G. L. Snider, and M. S. Shur, Appl. Phys. Lett. **72**, 707 (1998).
[18] M. S. Shur and M. Asif Khan, MRS Bull. **22**, 44 (1997).